Molecular Crystals and Liquid Crystals
Publication details, including instructions for authors and subscription information:
http://www.tandfonline.com/loi/gmcl20

Layered Double Hydroxide Intercalated with Sodium Dodecyl Sulfate

Lumbidzani Moyo [a], Walter W. Focke [a], Frederick J. W. J. Labuschagne [a] & Sabine Verryn [b]

[a] Institute of Applied Materials, Department of Chemical Engineering, University of Pretoria, Lynnwood Road, Pretoria 0002

[b] Institute of Applied Materials, Department of Geology, University of Pretoria, Lynnwood Road, Pretoria, 0002

Available online: 14 Feb 2012

To cite this article: Lumbidzani Moyo, Walter W. Focke, Frederick J. W. J. Labuschagne & Sabine Verryn (2012): Layered Double Hydroxide Intercalated with Sodium Dodecyl Sulfate, Molecular Crystals and Liquid Crystals, 555:1, 51-64

To link to this article: http://dx.doi.org/10.1080/15421406.2012.634366

Mol. Cryst. Liq. Cryst., Vol. 555: pp. 51–64, 2012

ISSN: 1542-1406 print/1563-5287 online
DOI: 10.1080/15421406.2012.634366

Taylor & Francis
Taylor & Francis Group

Layered Double Hydroxide Intercalated with Sodium Dodecyl Sulfate

LUMBIDZANI MOYO,[1] WALTER W. FOCKE,[1,*]
FREDERICK J. W. J. LABUSCHAGNE,[1]
AND SABINE VERRYN[2]

[1]Institute of Applied Materials, Department of Chemical Engineering, University of Pretoria, Lynnwood Road, Pretoria 0002
[2]Institute of Applied Materials, Department of Geology, University of Pretoria, Lynnwood Road, Pretoria 0002

The study investigates the intercalation of magnesium-aluminum layered double hydroxide with sodium dodecyl sulfate. Monolayer intercalation of the LDH-carbonate was achieved using an acetic acid-assisted ion exchange reaction. The carboxylic acid is believed to assist intercalation of dodecyl sulfate by facilitating the elimination of the carbonate ions present in the anionic clay. Bilayer intercalation was achieved by a coprecipitation method and this resulted in a highly crystalline product. However, in this case the interlayer contains a mixture of dodecyl sulfate anion, sodium dodecyl sulfate and the hydrolysis product dodecanol. The organic phase in the latter product shows an order-disorder transition between 100°C and 120°C, with thermal degradation and volatilization commencing above 170°C.

Keywords Anionic surfactant; intercalation; ion exchange reconstruction; layered double hydroxide

Introduction

Mg-Al layered double hydroxides (LDH) are anionic clays with the general formula $[Mg_{1-x}Al_x(OH)_2]^{x+}A^{y-}_{x/y}.\,n\,H_2O$. Here A denotes the charge balancing anion and the fractional aluminum substitution in the layers usually varies in the range $0.2 < x < 0.36$ [2–7]. The three dimensional structure of the clay is maintained by a combination of electrostatic forces and hydrogen bonding interactions between the layer and interlayer anions or molecules [7]. Carbonate ions in particular, interact strongly with both clay surfaces via hydrogen bonding forces [8,9]. Hydrophobic interactions also play a role when the inserted anions contain long aliphatic chains [10–12].

Intercalation may be regarded as a form of spontaneous self assembly comprising a 'reversible insertion of mobile guest species into a crystalline host lattice during which the structural integrity of the latter is formally conserved' [13,14]. The insertion of anionic surfactants functionalizes the clay, converting the hydrophilic nature of the interlayer into a hydrophobic one. Consequently, additional non-polar and low-water-soluble organic

*Address correspondence to Walter W Focke, Institute of Applied Materials, Department of Chemical Engineering, University of Pretoria, Lynnwood Road, Pretoria 0002. Tel.: +27 12 420 3728; Fax: + 27 12 420 2516; E-mail: walter.focke@up.ac.za

molecules may be absorbed into the interlayer. This improves the interaction of the clay with polymer matrices and hence facilitates the formation of polymer–clay nanocomposites [15].

Several studies reviewed surfactant intercalation into LDH [16,17,18]. Crepaldi et al. [19] identified three main intercalation techniques i.e.: (i) direct anion exchange; (ii) LDH reconstruction from a layered double oxide form obtained by calcinations of a suitable precursor; and (iii) anion replacement by elimination of the precursor interlamellar species. Intercalated LDH's can also be prepared by direct synthesis methods, e.g. hydrothermal crystallization of gels formed by the coprecipitation of the M^{2+} and M^{3+} hydroxides in the presence of the required organic anion [12,16,19,20–22].

Layered double hydroxide lattices can adapt to the geometry of the inserted guest species by adjustment of the interlayer separation. Intercalation of organic compounds creates diverse types of supramolecular structures in the clay interlayer [23]. Linear surfactant molecules with appropriate functional groups self-assemble between the LDH sheets into either monolayers or bilayers [13]. The monolayers comprise two interdigitated anti-parallel half-monolayers [12,24]. Anions within the interlayer will arrange themselves in such a manner as to maximize their interaction with the positive layer charge. Other factors, that affect the orientation of anionic surfactants such as dodecyl sulfate, are intercalation pH [20,21], the Mg:Al ratio [21] and the method of synthesis [17].

The intercalated alkyl chains assume a tilt with respect to the layer planes in order to facilitate their close packing [12,21]. The anti-parallel arrangement in monolayer intercalation also reduces the electrostatic repulsion between the anion head groups and effectively maintains the hydrophobic interactions between the hydrocarbon chains. A tilt angle of 60° was observed for alkyl sulfonates in Mg_2Al-LDH [25] while for alkyl sulfates in Zn_2Cr-LDH respectively it was 68.8° [4]. These values are somewhat higher than the expected "paraffin" angle of 56° [12].

The literature records a considerable spread in the basal spacing values [4,17,26,27]. Clearly the observed d-spacing of LDH-CO_3 and other intercalated derivatives depends on a number of factors. Much of the variation can be attributed to differences in the degree of hydration, i.e. the presence or absence of interlayer water. This explains the variations induced by different drying procedures and drying temperatures. Meyn et al. [26] indicates that vacuum drying at 65°C reduces the basal spacing by about 0.3 nm owing to removal of the adsorbed water from the interlayer. The chain structure i.e. chain length and cross section, also determines the packing of anions within the interlayer. The formation of kinks in intercalated alkyl chains may result in deviations in the d-spacing [4]. The aliphatic chain tilt angle may even be affected by the presence of the interlayer water [27]. Zhao and Nagy [21] state that the intercalation pH influences the d-spacing of intercalates prepared by the coprecipitation method. Clearfield et al. [20] found that, as the exchange pH was increased, so did the basal spacing although, surprisingly, the amount of sodium dodecyl sulfate (SDS) in the interlayer decreased. This study provides new experimental evidence that provides an explanation for this counterintuitive result.

The carbonate anions in LDH-CO_3 do not readily ion exchange owing to strong hydrogen-bonding interactions in addition to the electrostatic forces. Iyi et al. [29] showed that the conversion of LDH-CO_3 into LDH-A, where A is another inorganic anion, is facilitated by the presence of dilute acids functioning as decarbonation aids. Moyo et al. [18] extended this approach to the intercalation of LDH-CO_3 with dodecyl sulfate (DS) and dodecylbenzenesulfonate (DBS). They used water-soluble organic acids, e.g. acetic, butyric or hexanoic acid, to aid decarbonation of LDH-CO_3 [18]. It was found that the intercalation proceeded smoothly under mild conditions of pH and temperature when water soluble

carboxylic acids were added to aqueous suspensions LDH-CO_3 and surfactant. The carboxylic acids are believed to assist intercalation by facilitating the elimination of the carbonate ions present in the anionic clay galleries. Compared to the regeneration approach, well crystallized monolayer products with improved purity were obtained [18]. In this way monolayer intercalated LDH-DS of reasonable purity and high crystallinity was prepared from LDH-CO_3.

The regeneration method has also been used to replace carbonate with other guest ions, e.g. anionic surfactants. In this method the LDH-CO_3 is heated and converted into an essentially carbonate-free layered double oxide. This product is then suspended and stirred in aqueous medium containing the desired anion. This study showed that, while the method works for dodecylbenzenesulfonate (DBS), problems are encountered when applying it to dodecyl sulfate (DS). The latter surfactant tends to hydrolyze in highly basic media to form sulfate ions and dodecanol. Thus LDH-DS prepared by the regeneration method also contains LDH-SO_4 as an impurity. Furthermore, Moyo et al. [18] postulated that the liberated dodecanol may co-intercalate with DS in a bilayer format to give an additional impurity phase. They used this hypothesis to explain anomalous d-spacing reported for LDH-DS by other investigations [17,20,21,28,29,30,31]. This communication provides experimental proof for the existence of such a phase. It reports on the synthesis and characterization of a bilayer phase formed by co-intercalation of sodium dodecyl sulfate, dodecyl sulfate and dodecanol in LDH. The novelty here is that the alcohol is not purposefully added but is generated in situ via the hydrolysis of the surfactant.

Experimental

Materials

LDH-CO_3 (Hydrotalcite Grade HT 325) was supplied by Chamotte Holdings. It contained silica and magnesium carbonate as minor impurities. Distilled water was used in all experiments. High purity (>98%) sodium dodecyl sulfate (SDS) was purchased from Fluka-Biochemika. AR grade glacial acetic acid and acetone (99.5%) were supplied by Saarchem UnivAR. 25% aqueous ammonium hydroxide solution was procured from Promark chemicals. Magnesium nitrate ($Mg(NO_3)_3{\cdot}6H_2O$) and aluminum nitrate ($Al(NO_3)_3{\cdot}9H_2O$) were obtained from Merck with a purity of >92% and ≥98.5% respectively. Potassium bromide (Uvasol KBr, Merck) was used for prepare samples for FTIR spectra recording.

Sample Preparation

The preparation of LDH-DS (monolayer intercalated product) from the carbonate form was previously reported by Moyo et al. [18]. The composition of the precursor carbonate, Grade HT-325, is approximately $[Mg_{0.66}Al_{0.34}(OH)_2](CO_3)_{0.17}{\cdot}\frac{1}{2}H_2O$. 75 g sodium dodecyl sulfate (SDS) (0.26 mol) and 15 g acetic acid (0.25 mol) were dispersed in 1.5 L distilled water and the pH adjusted to pH = 10. 20 g LDH-CO_3 (ca. 0.10 mol Al) was added slowly while stirring. The suspension was left to stir overnight. The pH was again adjusted to pH = 10 each morning by adding dilute ammonia or NaOH solution if required. It was noted that pH dropped to as low as pH = 7.2 overnight. The mixture was allowed to react at ambient temperature for a total of two days. The product was recovered by centrifugation, washed four times with distilled water, and once with acetone. After each washing the solids were separated from the liquid by centrifugation. The product was allowed to dry at room temperature.

The LDH-SDS (co-intercalated sample) was prepared by a co-precipitation procedure. Different pH and reaction temperatures were tried but the following procedure gave a highly crystalline, X-ray pure phase. First, 51.8 g magnesium nitrate and 38.1 g aluminum nitrate were dissolved in 300 ml of deionised water. An amount of 57.9 g of SDS was dispersed in 500 ml of deionised water and then added to 300 ml of a NaOH solution (pH = 10). This mixture was stirred until a clear solution was obtained. The mixed metal nitrates solution was then added drop-wise under continuous stirring. After addition of the mixed metal nitrates it was found that the pH had dropped to pH = 5 and this was corrected to pH = 8 ± 0.5. The dispersion was left to stir under an inert atmosphere for 36 h and then aged at 65°C for 24 h. The precipitated solid was recovered by centrifugation. It was washed four times with water and left to oven dry at 65°C.

Characterization

Powder samples were viewed on a JEOL 840 SEM scanning electron microscope under low magnification. Sample preparation was as follows: A small quantity of the powder products or the LDH-CO_3 precursor was placed onto carbon tape on a metal sample holder. Excess powder was removed using a single compressed air blast. The samples were then coated five times with gold under argon gas using the SEM autocoating unit E5200 (Polaron equipment LTD).

Thermogravimetric analysis was conducted on a Mettler Toledo A851 TGA/SDTA machine. Powder samples of ca. 10 mg were placed in 70 μL alumina open pans. Temperature was scanned at 10°C/min in air range from 25°C to 1200°C. Further analysis was carried out on a Thermo Scientific VersaTherm TG coupled with a FTIR to follow the degradation of the samples. A 10 to 20 mg of sample was placed in quartz pans. The temperature was scanned from 30°C to 1000°C at 10°C/min in air at a flow rate of 50 mL/min. The gases evolved were analyzed using a Nicolet 470 FT-IR spectrophotometer.

FTIR spectra were recorded on a Perkin Elmer 100 Spectrophotometer. Samples were finely ground and combined with spectroscopic grade KBr in a ratio of 1:50, i.e. approximately 2 mg of sample and 100 mg of KBr. The mixture was pressed into a 13 mm ϕ die pellet. The reported spectra were obtained over the range 400–4000 cm^{-1} and represent the average of 32 scans at a resolution of 2 cm^{-1}. In the case of the temperature scan FT-IR, a small amount of sample was sandwiched between 13 mm diameter KBr disks and placed into the temperature-controlled sample holder. The temperature was increased at a rate of 10°C/min between temperature settings. On reaching a measurement setting, the sample was allowed to equilibrate for one minute before recording the spectrum.

Differential scanning calorimetry data were collected from a DSC TA Q2000 instrument. Approximately 5 to 10 mg of sample was placed in an aluminum pan. A pin hole was made in the lid. The sample was heated from to the required end temperature, e.g. 400°C at a scan rate of 10°C/min and in a N_2 flow rate of 50 mL/min.

Phase identification was carried out by XRD analysis on a PANalytical X-pert Pro powder diffractometer. The instrument features variable divergence and receiving slits and an X'celerator detector using Fe filtered Co K-α radiation (0.17901 nm). The X'Pert High Score Plus software was used for data manipulation. The temperature scan XRD data were obtained on the same machine using an Anton Paar HT16 heating chamber with Pt-heating filament. Silicon powder (Aldrich 99% purity) was mixed with the sample for calibration of results prepared for XRD analysis using back a loading preparation method. Samples were measured between $2\theta = 1^\circ$ and $2\theta = 40^\circ$ in heating mode at preselected temperatures with a waiting time of 1 minute and measurement time of 6 minutes per scan. The data were

corrected for sample displacement using X'Pert Highscore plus software. It is presented as variable slit data as that allows for better data visualization.

Inductive Coupled Plasma Optical Emission Spectroscopy (ICP-OES) analysis was carried out on a Perkin Elmer Optima 5300 DV. The major elements present were determined by analyzing solutions obtained by fusing the sample with sodium peroxide and then leach it with 6% hydrochloric acid. Elemental analysis (C, H, N & S) was done using a Carlo Erba NA 1500 C/N/S analyzer. Initially, C and S were determined in the C, N and S configuration. The instrument in the C and N configuration was modified to determine H as well, and a few days later this was used for C & H determination.

Results and Discussion

Figure 1 shows SEM micrographs of the two intercalates. The LDH-DS powder consists of agglomerated platelets that are similar in size to those seen in the precursor. LDH-SDS featured large crystallites with three different growth habits, ranging from plain platelets to bars, ribbons and even wire-like forms. Xu & Braterman [12] observed similar crystal growth habits in LDH-DBS and explain these differences in terms of intermolecular interactions in surfactant intercalated LDHs [31]. These 1-D morphologies are as a result

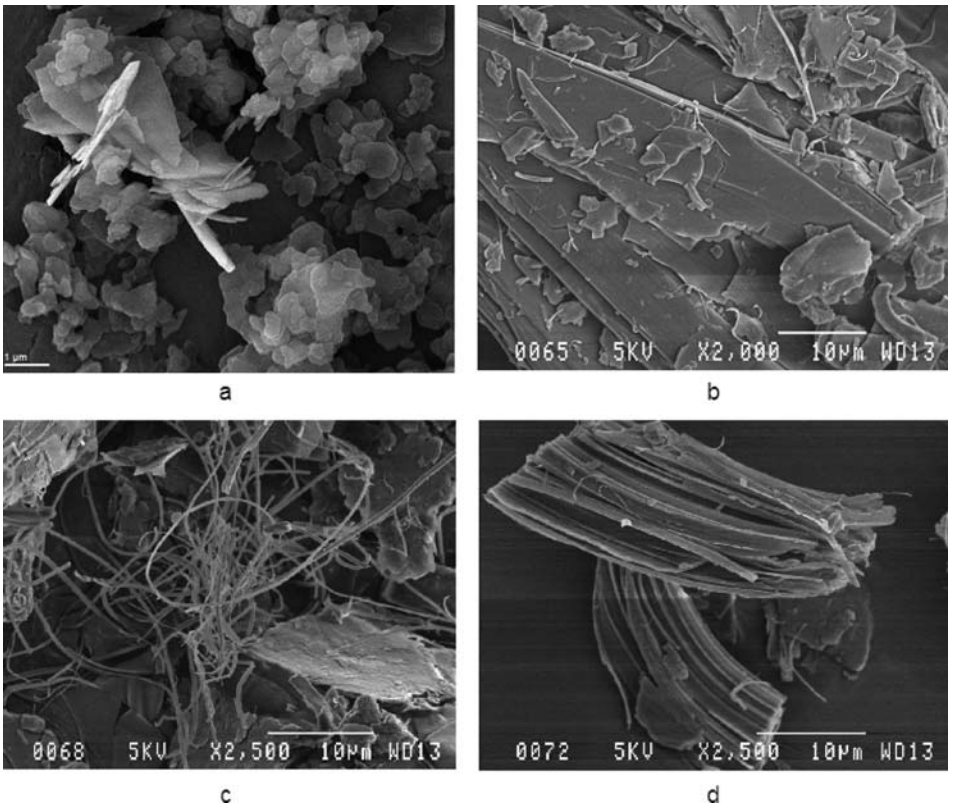

Figure 1. SEM micrographs of the crystal habits observed for (a) LDH-DS the product prepared by acetic acid aided intercalation, and (b) to (d) LDH-SDS, the product obtained by the coprecipitation method.

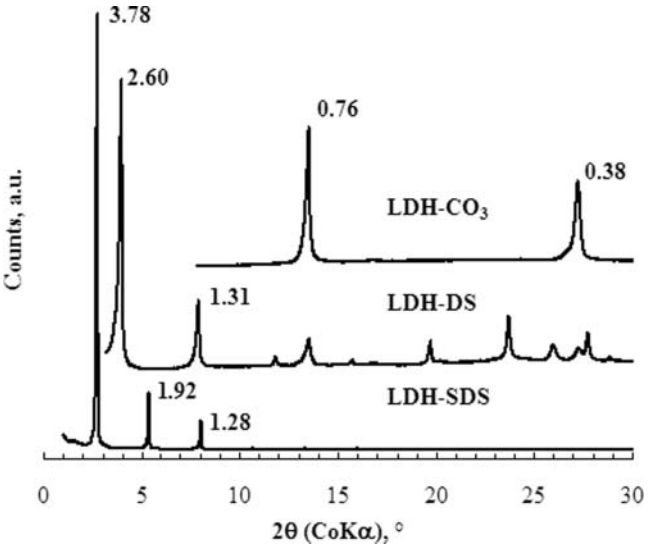

Figure 2. Powder XRD diffractograms for LDH-CO_3, LDH-DS the product prepared by acetic acid aided intercalation, and LDH-SDS, the product obtained with the coprecipitation method. Basal spacing values are indicated in nm.

of preferential crystal growth in the stacking direction i.e. c-axis [32]. The fibrous structure arises from the external layers of the LDH folding hence forming a mesostructured material through the formation of a small number of Al-O-Al groups [32,33]. The twists and bends, that the ribbon-like particles exhibit, originate from the hydrophobic interactions between the internal and external surfactant anions.

Figure 2 compares the X-ray diffractograms recorded for LDH-CO_3, LDH-DS (prepared in the presence of acetic acid) and the LDH-SDS prepared by coprecipitation. The characteristic reflections for LDH-CO_3 found at 0.762 nm ($2\theta = 13.5^\circ$) and 0.38 nm ($2\theta = 27.2^\circ$) are also observed in the diffractogram for LDH-DS, indicating its presence as an impurity. The peak at 11.8° (basal spacing 0.87 nm) is consistent with the presence of LDH-SO_4 as an additional impurity in the LDH-DS phase [34,35]. The observed basal spacing for LDH-DS equals $d_L = 2.62$ nm and this is consistent with monolayer intercalation [18]. Similar basal spacing values were reported for LDH-DS prepared by other methods [21, 28, 34, 30, 36-39]. These results confirm that the lower aliphatic acids facilitate intercalation of SDS into LDH-CO_3 under mild conditions, e.g. aqueous medium at ambient temperature and pH < 10. None of the above-mentioned reflections are found in the XRD spectrum for the LDH-SDS coprecipitation product. The LDH-SDS basal spacing of $d_L = 3.78$ is characteristic of a bilayer intercalation. XRD peak broadening arises from strain and defects within the crystallites [31]. However, the peaks in the LDH-SDS diffraction pattern are narrow and symmetrical indicating a high degree of ordering. The greater degree of crystal perfection obtained with the coprecipitation method shows the advantage of direct formation of the LDH-surfactant from solution above the transformation of a pre-existing solid [31]. Note that the XRD results indicate a single crystalline phase despite the variety of crystal habits observed with SEM.

Figure 3 shows FTIR spectra of the vapor released at selected temperatures in the TG-FTIR scan for LDH-SDS. Alkyl bands appear at 175°C owing to the onset of thermal

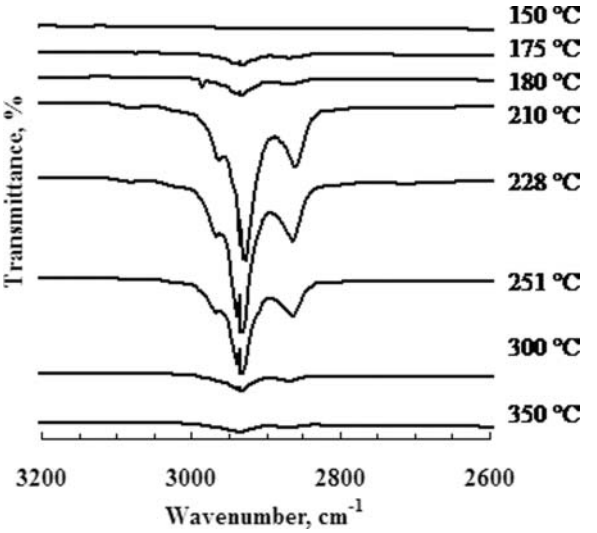

Figure 3. FTIR spectra of the vapor released from LDH-SDS obtained by TG-FTIR at a scan rate of 10°C/min in an air atmosphere. It shows that thermal degradation of the surfactant commences at ca. 175°C and is virtually complete by 300°C.

degradation and volatilization of the surfactant. The bands increase in strength as the temperature is increased to 228°C, beyond this temperature they wane so that at 300°C and 350°C only weak absorptions are observed. Absorption bands associated with sulfate or sulfur oxides were not observed in this temperature range suggesting that the sulfate functional group is largely retained in the inorganic residue.

Table 1 presents composition data for the precursor LDH-CO_3 and the intercalated products. The ICP data are reported as atom ratios relative to aluminum. The elemental analysis data are reported as atom ratios relative to sulfur. The composition of the carbonate can be represented by the formula $[Mg_{1-x}Al_x(OH)_2](CO_3)_{x/2}.nH_2O$ with the quantity x quantifying the fractional replacement of Mg by Al in the clay sheets. The data for the intercalated compounds is consistent with $[Mg_{1-x}Al_x(OH)_2]\{DS_x \cdot NaDS_y \cdot DOH_z\} \cdot nH_2O$. This formula implies that the clay galleries are occupied by a mixture of chains corresponding to the DS anion, its sodium salt as well as the alcohol hydrolysis product, dodecanol (DOH). The sodium content of the intercalated clay is accounted for by the quantity y. The value of z was determined from the carbon-sulfur ratio taking cognizance of the fact that it should equal 12 if no hydrolysis occurred. The degree of intercalation of alkyl chains in the galleries

Table 1. Composition data for LDH-CO_3, LDH-DS and LDH-SDS samples. ICP and elemental analysis data are presented as atom ratios relative to aluminum and relative to sulfur respectively

Compound	Mg/Al	Na/Al	C/S	x	y	z
LDH-CO_3	1.99	0.06	—	0.34	0	0
LDH-DS	1.98	0.01	12.5	0.34	0.00	0.02
LDH-SDS	1.82	1.28	18.7	0.35	0.46	0.45

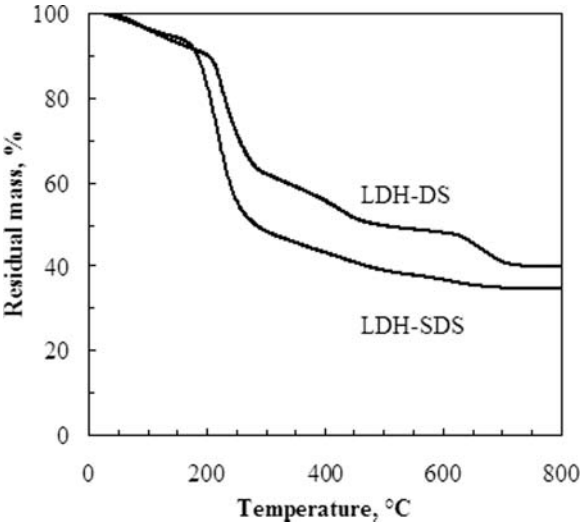

Figure 4. Thermogravimetric (TG) mass loss curves for LDH-SDS, the product obtained by the coprecipitation method obtained at a scan rate of 10°C/min in an air atmosphere.

can be expressed as a ratio relative to the anion exchange capacity as determined by the quantity x. Table 1 lists the values of x, y and z determined from the composition data. The number of intercalated chains per formula repeat units is simply the sum of the quantities x, y and z. So the ratio equals $(x + y + z)/x$. Thus the degree of intercalation is 1.07 and 3.55 for the LDH-DS and LDH-SDS respectively. Similar high degrees of intercalation values were previously observed for LDH-stearate [40].

Figure 4 shows the thermogravimetric traces for LDH-DS and LDH-SDS, both feature several thermal decomposition events below 800°C. The first step is attributed to loss of interlayer water and is assumed complete at a temperature of about 150°C [41–44]. The second and strongest event is characterized by a very pronounced derivative TG peak centered at ca. 225°C in both compounds. This mass loss corresponds to the thermal degradation of the organic intercalants as proven by the TG-FTIR results. Mass loss is effectively complete at 800°C. However, it is conceivable that the inorganic sulfates formed during thermal degradation, will decompose at even higher temperatures.

The expected mass loss can be estimated using the reaction shown in Scheme 1. It assumes that the decomposition of the surfactant liberates volatile alkyl fragments and that the residue, (corresponding to the plateau the values reached at 800°C in the TG traces of Fig. 3) comprises anhydrous inorganic sulfate salts and metal oxides. According to Scheme 1, the expected residue amounts are 43.9 wt% and 32.6 wt% for the present

$$[Mg_{1-x}Al_x(OH)_2]\{DS_x \cdot NaDS_y \cdot DOH_z\} \cdot 0.5H_2O$$

$$\rightarrow (2\text{-}4x\text{-}y)/2\ MgO + y/2\ Na_2SO_4 + (2x+y)/2\ MgSO_4 + x/2\ Al_2O_3$$

Scheme 1. Idealized thermal decomposition route for LDH-SDS showing only the solid residue

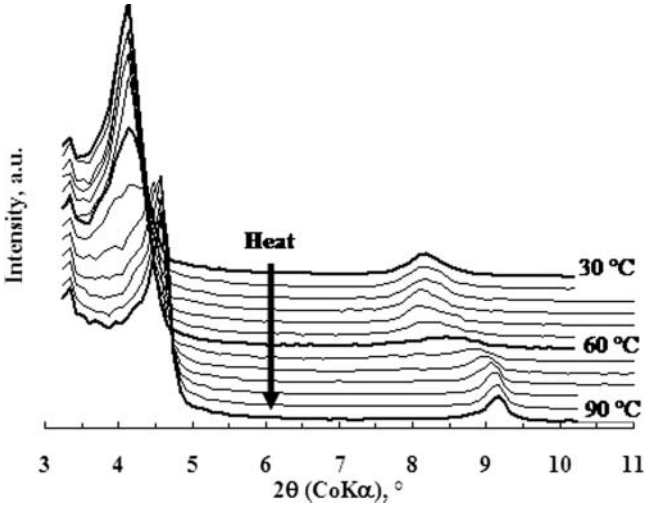

Figure 5. The effect of temperature on the X-ray diffractograms of LDH-DS after vacuum drying. Traces are plotted at 5°C temperature intervals. A transition from a d-spacing of 2.48 nm to 2.24 nm occurs around 60°C.

LDH-DS and LDH-SDS samples respectively. The observed values of 40.0 wt% and 34.9 wt% respectively deviate somewhat from these predictions.

Figures 5 and 6 show XRD diffractograms obtained at increasing temperatures in air for LDH-DS and LDH-SDS respectively. In both cases the basal reflection, corresponding to the crystalline phase, first shows a shift to larger 2θ angles at a characteristic temperature. At much higher temperatures the peaks disappear completely, indicating amorphization.

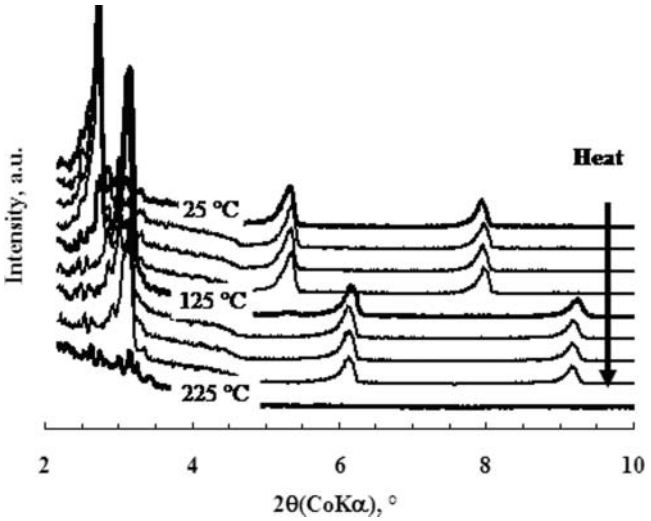

Figure 6. The effect of temperature on the X-ray diffractograms of LDH-SDS, the product obtained by the coprecipitation method. Traces are plotted at 25°C temperature intervals. Between 100°C and 125°C the d-spacing decreases from 3.78 nm to 3.27 nm.

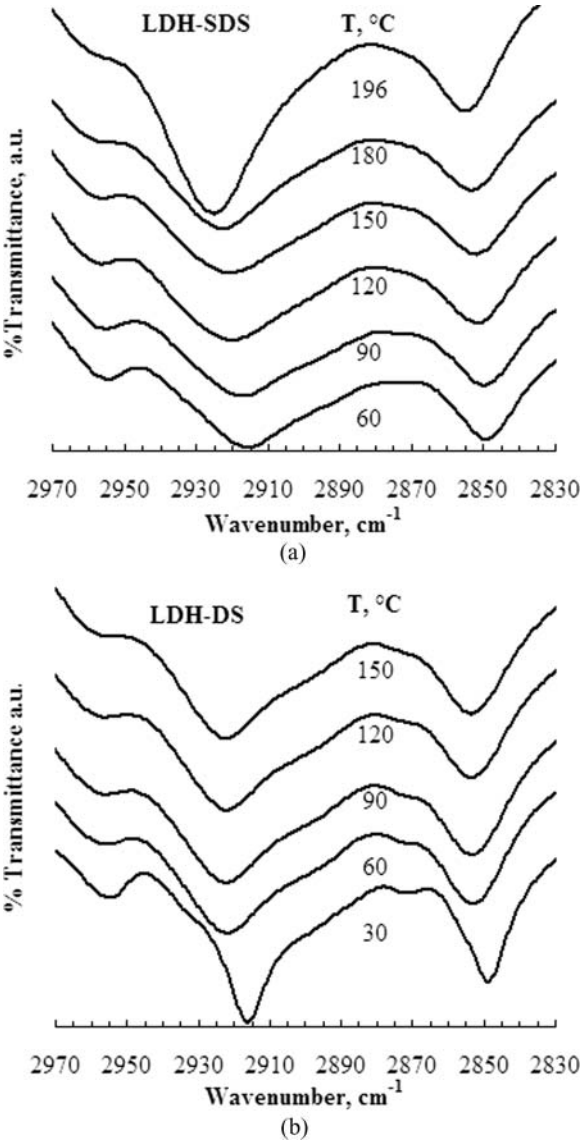

Figure 7. The effect of temperature on the FT-IR spectra for LDH-DS and LDH-SDS.

The observed shift at intermediate temperatures is indicative of a reduction in the d-spacing, i.e. the clay layers coming closer together. Such a decrease in the basal spacing can, at least in part, be attributed to the loss of physisorbed and intercalated water [27].

FTIR spectra recorded at increasing temperatures for the LDH-SDS are shown in Fig. 7. Strong bands are featured near $\sim$2920 cm^{-1} and $\sim$2850 cm^{-1} regions. These result from the CH_2 asymmetric $\nu_{as}(CH_2)$, and symmetric $\nu_s(CH_2)$ stretch modes, respectively. Vaia et al. [45] proposed the use of the $\nu_{as}(CH_2)$ band to investigate the state of the chains in the interlayer region. The wavenumber and the width of this band are sensitive to the gauche/trans conformer ratio and the packing density of the chain methylenes. It varies from 2918 cm^{-1}

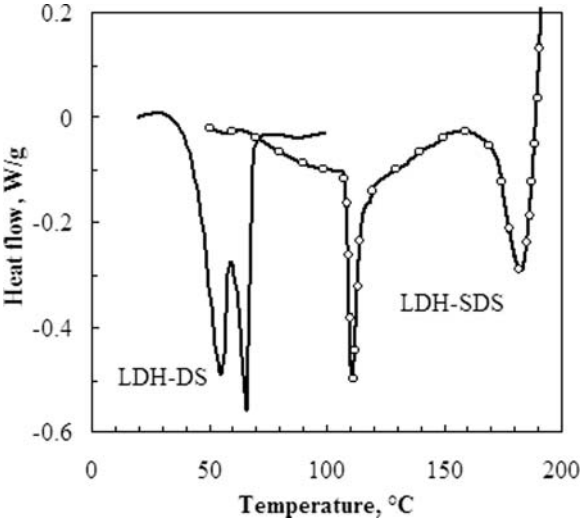

Figure 8. DSC melting endotherms of LDH-DS and LDH-SDS obtained at a scan rate of 10°C/min in an air atmosphere.

for the methylene chains in the all-trans ordered state in a crystalline surfactant to 2929 cm^{-1} when the chains are in a liquid-like state [45,46]. The peak positions of the methylene asymmetric bands in Figure 7 show a gradual shift from ca. 2914 cm^{-1} to 2924 cm^{-1} as the temperature increases from 25°C to above 180°C. This indicates a transition from an ordered crystalline state to a liquid-like state. A similar change is observed for LDH-DS except that in this case a more sudden shift is indicated that is complete by ca. 60°C.

Figure 8 shows the DSC trace responses for the LDH-SDS and LDH-DS samples. Unlike the more gradual transition indicated by the FTIR data, the DSC reveals two sharp endothermic events in LDH-DS. These are interpreted as a rotator phase transition of the alkyl chains. In LDH-SDS the measured enthalpy is ca. 51 kJ/kg. This is equivalent to ca. 139 kJ/kg dodecanol radicals intercalated. The enthalpy of melting for pure dodecanol is 200 kJ/kg, i.e. just about 44% higher. Pure dodecanol melts at ca. 26°C but the two peaks are located at much higher temperatures, i.e. 55°C and 66°C. The higher transition temperature is caused by the anchoring of the dodecanol radicals via the sulfate head groups and by the two-dimensional confinement imposed by the clay sheets.

The DSC trace for LDH-SDS shows only a single endothermic peak at the significantly higher temperature of 111°C apart from the endothermic decomposition event above 160°C. In this case the enthalpy change is at least 18 kJ/kg but an accurate determination of the enthalpy is difficult owing to an ill-defined baseline. However, this peak is also attributed to a rotator-like phase transition. This is supported by the hot stage microscopy images shown in Figure 9. They show that the crystals are still physically intact at 130°C. At much higher temperatures (198°C) the residue looks like molten droplets. The DSC, FTIR and XRD data all indicate that the rotator phase transition occurs at significantly lower temperatures in the monolayer intercalated LDH-DS than in the bilayer intercalated LDH-SDS.

The following explanation is offered to explain why single layer intercalation is obtained in the one instance and double layer intercalation in the other. LDH clays feature a relatively high charge density. Dense close-packing of the surfactants in the galleries

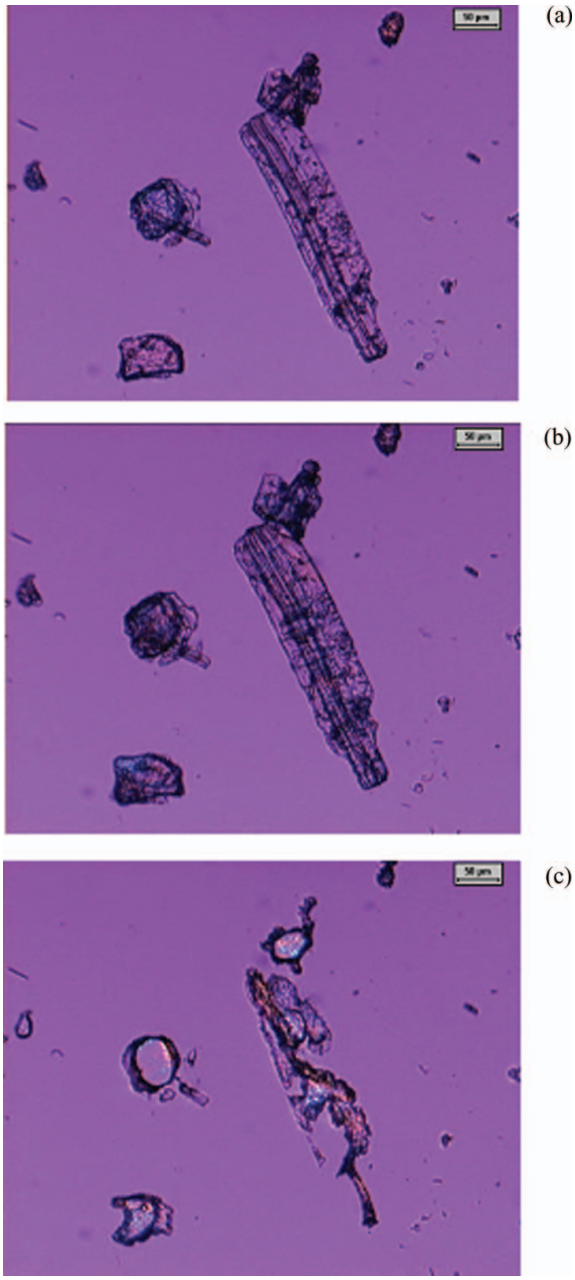

Figure 9. Hot stage images of the LDH-SDS recorded at temperatures of (a) 38°C, (b) 130°C, and (c) 198°C.

improves the van der Waals interactions between long alkyl chains. However, this requires charge shielding of the same-charge surfactant head groups. Close packing of chain extended surfactants can be facilitated in two distinct ways. The electrostatic repulsion between the anionic head groups can be minimized by interdigitated intercalation with

adjacent surfactant molecules are assembled in such a way that the polar heads face opposite directions. This is what happens in the absence of the long chain alcohol molecules. However, co-intercalated alcohols placed in-between adjacent surfactant molecules appear to provide sufficient electrostatic shielding to allow bilayer intercalation with the head groups in each layer facing the clay sheets.

Conclusions

The direct intercalation of surfactants in LDH-CO_3 is difficult due to high affinity of carbonate anions to the positive charge of the hydroxide layer. The elimination method employs short chain carboxylic acids to facilitate the intercalation of SDS. They assist with the expulsion of the carbonate anion without becoming co-intercalated. The resultant organo-LDH is a monolayer intercalated LDH-DS. In contrast LDH-SDS produced by co-precipitation can form a bilayer arrangement when part of the surfactant is allowed to hydrolyze. At favorable pH conditions, alternately low and then relatively high, an environment favorable for in-situ generation of dodecanol is created. This then co-intercalates with the dodecyl sulfate ions and its sodium salt. Both the monolayer and the bilayer products show a "rotator" phase transition at elevated temperatures. Interestingly, this transition occurs at a much higher temperature in the bilayer-intercalated product (111°C) than in the monolayer-intercalated product (ca. 60°C). At temperatures above ca. 175°C, both systems thermally degrade releasing alkyl fragments and form an amorphous solid residue phase.

Acknowledgments

This work is based on research supported by the National Research Foundation (NRF) through the Institutional Research Development Programme (IRDP) and the South Africa/Germany Research Collaboration Programme. Financial support from NRF and also from the Bundesministerium für Forschung (BMF) is gratefully acknowledged.

References

[1] Miyata, S., & Kumura, T. (1973). *Chem. Lett.*, 843.
[2] Brindley, G. W., & Kikkawa, S. (1979). *Am. Mineral.*, *64*, 836.
[3] Miyata, S. (1980). *Clays Clay Miner.*, *28*, 50.
[4] Kopka, H., Beneke, K., & Lagaly, G. (1988). *J. Colloid Interfac. Sci.*, *123*, 427.
[5] Reichle, W. T. (1986). *Solid State Ionics*. *22*, 135.
[6] Chibwe, K., & Jones, W. (1989). *J. Chem. Soc., Chem. Commun.*, 926.
[7] Cavani, F., Trifirò, F., & Vaccari, A. (1991). *Catal. Today*, *11*, 173.
[8] Labajos, F. M., Rives, V., & Ulibarri, M A. (1992). *J. Mater. Sci.*, *27*, 1546.
[9] Kloprogge, J. T., Wharton, D., Hickey, L. & Frost, R. L. (2002). *Am. Mineral.*, *87*, 623.
[10] Kanoh, T., Shichi, T., & Takagi, K. (1999). *Chem. Lett.*, 117.
[11] Itoh, T., Ohta, N., Shichi, T., Yui, T., & Takagi, K. (2003). *Langmuir*, *19*, 9120.
[12] Xu, Z. P., & Braterman, P. S. (2003). *J. Mater. Chem.*, *13*, 268.
[13] O'Hare, D. (1991). In: *Inorganic Materials*, Bruce, D. W. & O'Hare, D. (Eds.), New York: Wiley, 166.
[14] Messersmith, P. B., & Stupp, S. I. (1995). *Chem. Mater.*, *7*, 454.
[15] Utraki, L. A. (2004). *Clay-Containing Polymeric Nanocomposites*, Shropshire, UK: Rapra Technologies Ltd.
[16] Crepaldi, E. L., Pavan, P. C., Tronto, J., Cardoso, L. P., & Valim, J. B. (2002). *J. Colloid Interface Sci.*, *248*, 429.
[17] Newman, S. P., & Jones, W. (1998). *New J. Chem.*, 105.

[18] Moyo, L., Nhlapo, N. S., & Focke, W. W. (2008). *J. Mater. Sci.*, *43*, 6144.
[19] Crepaldi, E. L., Pavan, P. C., & Valim, J. B. (1999). *Chem. Commun.*, 155.
[20] Clearfield, A., Kieke, M., Kwan, J., Colon, J. L., & Wang, R. C. (1991). *J. Inclusion Phenom. Mol. Recognit. Chem.*, *11*, 361.
[21] Zhao, H., & Nagy, K. L. (2004). *J. Colloid Interface Sci.*, *274*, 613.
[22] Drezdzon, M. A. (1988). *Inorg. Chem.*, *27*, 4628.
[23] Dèkány, I., Berger, F., Imrik, K., & Lagaly, G. (1997). *Colloid. Polym. Sci.*, *275*, 681.
[24] Takagi, K., Shichi, T., Usami, H., & Sawaki, Y. (1993). *J. Am. Chem. Soc.*, *115*, 4339.
[25] Xu, Z. P., & Braterman, P. S. (2007). *J. Phys. Chem.*, *13*, 268.
[26] Meyn, M., Beneke, K., & Lagaly, G. (1990). *Inorg. Chem.*, *29*, 5201.
[27] Pesic, L., Salipurovic, S., Markovic, V., Vucelic, D., Kagunya, W., & Jones, W. (1992). *J. Mater. Chem.*, *2*(10), 1069.
[28] You, Y., Zhao, H., & Vance, G. F.,(2002a). *J. Mater. Chem.*, *12*, 907.
[29] Iyi, N., Okamoto, K., Kaneko, Y., & Matsumoto, T. (2005). *Chem. Lett.*, *34*, 932.
[30] Costa, F. R., Leuteritz, A., Wagenknecht, U., Jehnichen, D., Häusler, L., & Heinrich, G. (2008). *Appl. Clay. Sci.*, *38*(3-4), 153.
[31] Braterman, P. S., Xu, Z. P., & Yarberry, F. (2004). In: *Handbook of Layered Materials*, Auerbach, S. M., & Dutta, P. K. (Eds), New York: Taylor & Francis, 373.
[32] Hu, G., & O'Hare, D. (2005). *J. Am. Chem. Soc.*, *127*, 17808
[33] De Jesus Martinez-Ortiz, M., Lima, E., Lara, V., & Vivar, J. M. (2008). *Langmuir*, *24*, 8904
[34] Mascolo, G., & Marino, O. (1980). *Miner. Mag.*, *43*, 619.
[35] Miyata, S., & Okada A. (1977). *Clays Clay Miner.*, *25*, 14.
[36] Jobbágy, M., & Regazzoni, A. E. (2004). *J. Colloid Interface Sci.*, *275*, 345.
[37] Pavan, P. C., Crepaldi, E. L., & Valim, J. B. (2000). *J. Colloid Interface Sci.*, *229*, 346.
[38] Venugopal, B. R., Shivakumara, G., & Rajamathi, M. (2006). *J. Colloid Interface Sci.*, *294*, 234.
[39] Bouranda, M., Lafjah, M., Ouali, M. S., & De Menorval, L. C. (2008). *J. Hazard. Mater.*, *153*, 911.
[40] Nhlapo, N., Motumi, T., Landman, E., Verryn, S. M. C., & Focke, W. W. (2008). *J. Mater. Sci.*, *43*, 1033.
[41] Carlino, S., & Hudson, M. J. (1994). *J. Mater. Chem.*, *4*, 99.
[42] Evans, D. G., & Duan, X. (2005). *Chem. Commun.*, 485.
[43] Frost, R. L., Martens, W., Ding, Z., & Kloprogge, J. T. (2003). *J. Therm. Anal. Calorim.*, *71*, 429.
[44] Kandare, E., & Hossenlopp, J. M. (2006). *Inorg. Chem.*, *45*, 3766.
[45] Vaia, R., Teukolsky, R., & Giannelis, E. (1994). *Chem. Mater.*, *6*, 1017.
[46] Hongping, H., Ray, F. L., & Jianxi, Z. (2004). *Spectrochim. Acta*, *60*, 2853.